Collapse Moment Estimation of Wall Thinned Pipe Bends and Elbows by Simplified Cascaded Fuzzy Neural Networks

So Hun Yun [a], Young Do Koo [a], Man Gyun Na [a *]
[a]*Department of Nuclear Engineering, Chosun University, 309 Pilmun-daero, Dong-gu, Gwangju 61452, Korea*
[*]*Corresponding author: magyna@chosun.ac.kr*

1. Introduction

Nuclear power plants (NPPs) consist of numerous piping systems, where various pipe bends and elbows are used. These pipes are placed in proper locations in the piping system and carry out an important role in permitting the modification of the isometric routing and reducing the anchor reaction forces [1]. In addition, the pipe bends and elbows absorb energy through local plastic deformation under excessive load conditions above the elastic range, thereby preventing damage to the entire piping system.

However, in the piping system, the pipe bends and elbows are exposed to a large number of degradation mechanisms. When the pipe bends made of carbon steel are in contact with the fluid flow, there is a high possibility of occurrence of wall-thinned defects mainly by flow-accelerated corrosion (FAC) [2]. It is essential to investigate the effect of wall-thinned defects, since the wall thickness of the pipe bends and elbows under various loading conditions is likely to be thinned and broken.

Therefore, in this study, data on wall-thinned bends and elbows obtained through finite element method (FEM) were used to predict the collapse moment by using an artificial intelligence method. Then, the simplified cascaded fuzzy neural networks (SCFNNs) were used to estimate the collapse moments of the pipe bends and elbows in the piping system. Also, the related variables of SCFNN were optimized by the genetic algorithm combined with the least squares method and the SCFNN showed quite good performance.

2. Evaluation of the Collapse Moment using Finite Element Analyses

Using the FEM, the geometric shapes of the pipe bends and elbows of the piping system were modeled, and the collapse moment of this model was defined. Since the FEM has no restrictions on the use of load and boundary conditions, these conditions were treated as nodes.

2.1 Criteria for Collapse of Wall-thinned Pipe Bends and Elbows

The collapse moment (M_c) of the pipe bends and elbows in the piping system of the NPPs was obtained using the twice-elastic slope (TES) method from the moment (M) versus rotation curve (ρ), as shown in Fig.1 [1]. The collapse moments of the wall-thinned bends and elbows are defined as the intersection of the line corresponding to half the inclination of elastic region and the moment-rotation curve as shown in Fig. 1 (a). On the other hand, as shown in Fig. 1 (b), when the maximum moment appears at an angle smaller than the intersection of the moment-rotation curve and the TES line, the maximum moment is defined as the collapse moment. Here, parameter θ is half of the circumference angle of the wall-thinned defects and TES line is the straight line with 2θ angle on the vertical axis.

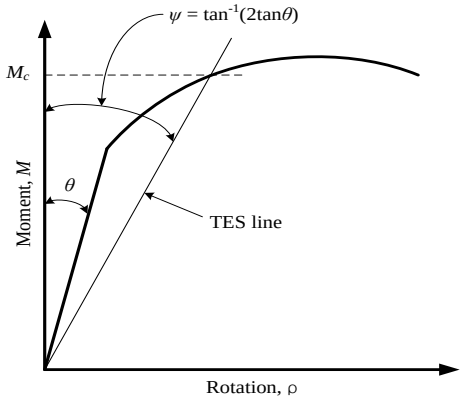

(a) Case 1

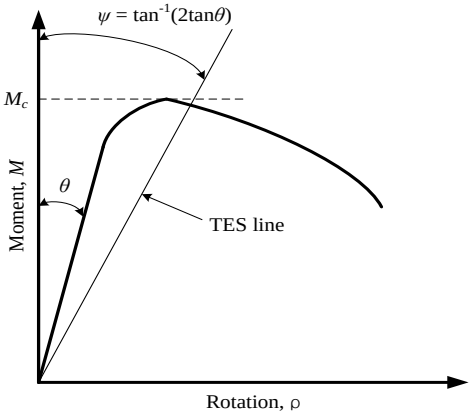

(b) Case 2

Fig. 1. Moment-Rotation curve [1]

2.2 Analysis Conditions

In order to analyze the behavior of the wall-thinned pipe bends and elbows with respect to the circumferential position of the defects, the carbon steel bends that have outer radius of 400mm and nominal

thickness of 20mm are considered. The pipe bends and elbows are connected to straight pipes with lengths equal to 10 times the mean radius (R_m) of the pipe bend to permit free ovalization of end section of the pipe ends. In this analysis, defects existing within the extrados, intrados and crowns of the pipe bend are assumed, and the geometry of the defects is as shown in Table I [1].

Table I: Conditions for FEA of Wall-thinned Pipe Bends and Elbows

Wall-thinned locations	Extrados, Intrados, Crown
Bend radius (R_b/R_m)	3, 6
Bend angle (°)	30°, 60°, 90°
Defect geometry	
Thinning length (L/D_o)	0.25, 0.5, 1.0, 1.5, 2.0
$(t_{nom}-t_p)/t_{nom}$	0.233, 0.466, 0.699
θ/π	0.0625, 0.125, 0.25, 0.50
Load	
Bending mode	Opening and closing
Pressure (MPa)	0, 5, 10, 15, 20

2.2 Finite Element Models

A nonlinear three-dimensional FEA was performed to evaluate the collapse moment at the wall-thinned bends and elbows. Because the geometry and load of the bend and elbow are symmetrical, an 1/2 symmetric model is used. And the FEA is accomplished using ABAQUS, a universal finite element analysis program.

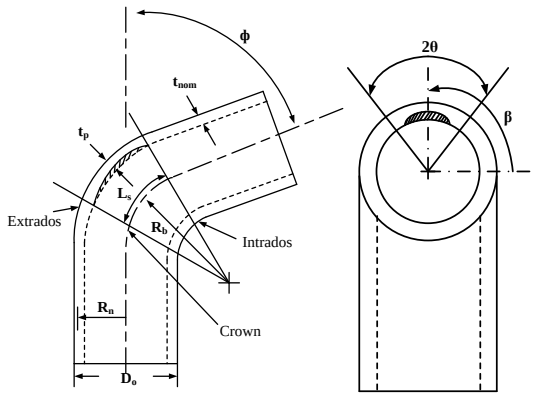

Fig. 2. Definition of dimensions for wall-thinned defects in pipe bends and elbows [1]

3. SCFNN methodology

3.1 CFNN Model

The FNN model is combination of a fuzzy inference system (FIS) and ANN's learning capability [3, 4]. The CFNN model have two or more FNN modules connected in series. Each single-stage FNN module consist of six layers, which contains fuzzy inference and training units. A single-stage FNN module will be described with Fig. 3. In this study, one of the fuzzy inference methods, the Takagi-Sugeno-type FIS was used. Using the Takagi-Sugeno-type FIS, an arbitrary i -th rule of each stage of the CFNN can be expressed as Eq. (1).

$$\begin{aligned}
&\text{Stage 1}\ \begin{bmatrix} x_1(k)\ is\ A_{i1}^1(k)\ AND\cdots AND\ x_m(k)\ is\ A_{im}^1(k), \\ then\ \hat{y}_1^i(k)\ is\ f_1^i(x_1(k),\cdots,x_m(k)) \end{bmatrix} \\
&\text{Stage 2}\ \begin{bmatrix} If\ x_1(k)\ is\ A_{i1}^2(k)\ AND\cdots AND\ x_m(k)\ is\ A_{im}^2(k), \\ AND\ \hat{y}_1(k)\ is\ A_{i(m+1)}^2(k), \\ then\ \hat{y}_2^i(k)\ is\ f_2^i(x_1(k),\cdots,x_m(k)),\ \hat{y}_1(k) \end{bmatrix} \\
&\quad\vdots \\
&\text{Stage g}\ \begin{bmatrix} If\ x_1(k)\ is\ A_{i1}^1(k)\ AND\cdots AND\ x_m(k)\ is\ A_{im}^1(k), \\ AND\ \hat{y}_1(k)\ is\ A_{i(m+1)}^g(k), AND\cdots AND\ \hat{y}_{(g-1)}(k)\ is\ A_{i(m+g-1)}^g(k), \\ then\ \hat{y}_g^i(k)\ is\ f_g^i(x_1(k),\cdots,x_m(k)),\ \hat{y}_1(k),\cdots,\hat{y}_{(g-1)}(k) \end{bmatrix}
\end{aligned} \tag{1}$$

where g indicates the stage number, $A_{ij}^g(k)$ is the membership function of the j -th input variable for the i -th fuzzy rule at the stage g ($i=1,\ 2,\cdots,\ n$; n is the number of fuzzy rules), and $\hat{y}_g^i(k)$ is the output of the i -th fuzzy rule at the stage g [4]. The i -th fuzzy rule at the stage g is expressed as Eq. (2).

$$\begin{aligned}
&f_g^i(x_1(k),\cdots,x_m(k),\hat{y}_1(k),\cdots,\hat{y}_{g-1}(k)) \\
&=\sum_{j=1}^{m} q_{ij}x_j+\sum_{j=1}^{g-1} q_{i(m+j)}\hat{y}_j+r_i
\end{aligned} \tag{2}$$

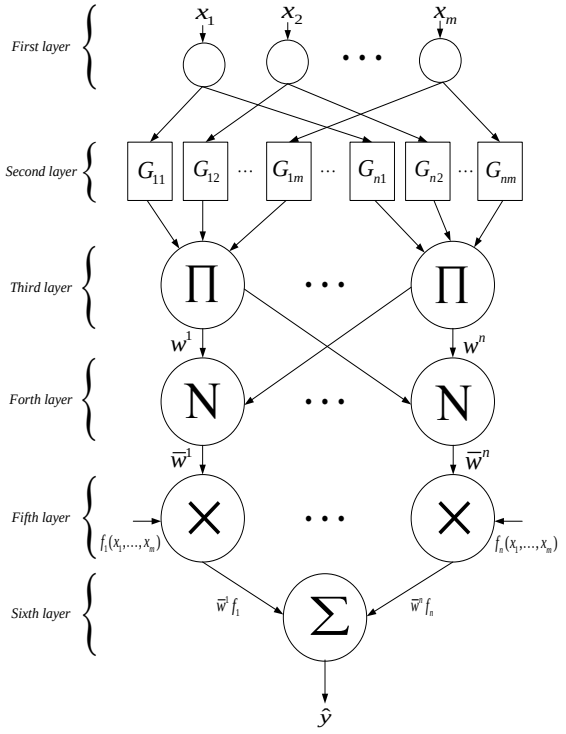

Fig. 3. First stage FNN module [4]

The output of the first stage FNN module using the Takagi-Sugeno-type can be expressed as Eq. (3).

$$\hat{y}(k) = \sum_{i}^{n} \overline{w}^{i}(k) f^{i}(x_1, \cdots, x_m) \tag{3}$$

where

$$A_{ij}(x_j(k)) = e^{-\frac{(x_j(k)-c_{ij})^2}{2s_{ij}^2}} \tag{4}$$

$$w^{i}(k) = \prod_{j=1}^{m} A_{ij}(x_j(k)) \tag{5}$$

$$\overline{w}^{i}(k) = \frac{w^{i}(k)}{\sum_{i=1}^{n} w^{i}(k)} \tag{6}$$

As shown in Fig. 3, the input values of the first layer are simply passed to the input of the next layer. Each node in the second layer implements membership function, and its output is the corresponding membership value of the input variable connected to it. A bell-shaped function is adopted in Eq. (4). The each node in third layer multiplies the membership function values from the second layer and the output of this layer is expressed as Eq. (5). And the fourth layer performs normalization using Eq. (6). The nodes of the fifth layer generate the output of each fuzzy *if-then* rule. Finally, the last layer aggregates all the fuzzy *if-then* rules and is expressed as Eq. (3) [4].

The output of the first FNN module is expressed as the vector product as shown in Eq. (7).

$$\hat{y}(k) = \mathbf{w}^{T}(k)\mathbf{q} \tag{7}$$

where

$$\mathbf{q} = [q_{11} \cdots q_{ni} \cdots q_{1m} \cdots q_{nm} r_1 \cdots r_n]^{T} \tag{8}$$

$$\begin{aligned}\mathbf{w}(k) = \big[& \overline{w}^{1}(k)x_1(k) \cdots \overline{w}^{n}(k)x_1(k) \cdots \overline{w}^{1}(k)x_m(k) \\ & \cdots \overline{w}^{n}(k)x_m(k)\overline{w}^{1}(k) \cdots \overline{w}^{n}(k)\big]^{T}\end{aligned} \tag{9}$$

The vector $\mathbf{q}$ is a consequent parameter vector that has $(m+1)n$ dimensions, and the vector $\mathbf{w}(k)$ is composed with input data and membership function values. The predicted outputs derived from Eq. (7) are expressed as Eq. (10) [4].

$$\hat{y} = \mathbf{W}\mathbf{q} \tag{10}$$

where

$$\hat{y} = [\hat{y}(1)\ \hat{y}(2) \cdots \hat{y}(L)]^{T},\ \mathbf{W} = [\mathbf{w}(1)\ \mathbf{w}(2) \cdots \mathbf{w}(L)]^{T} \tag{11}$$

3.2 Simplified CFNN Model

The SCFNN model is a simplified model of CFNN model. Only initial input data and the output value of the previous stage FNN module is applied to the next stage, as shown in Fig. 4. This process is repeated g times to optimize the output of the each FNN module. The SCFNN model simplifies complexly connected CFNN structures, leading to faster computations and similar performance.

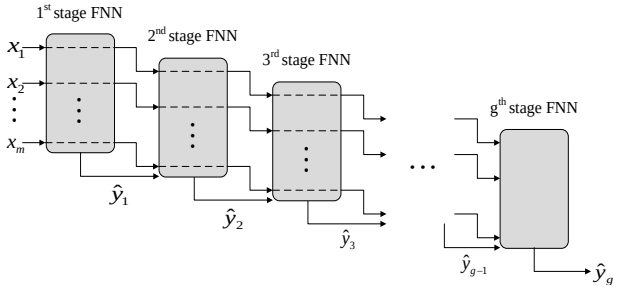

Fig. 4. Architecture of the SCFNN model

In the SCFNN model, the *if-then* rule of the stage *g* is expressed as Eq. (12).

$$\text{Stage g} \begin{bmatrix} \textit{If } x_1(k) \textit{ is } A_{1}^{1}(k) \textit{ AND} \cdots \textit{AND } x_m(k) \textit{ is } A_{1m}^{1}(k), \\ \textit{AND } \hat{y}_1(k) \textit{ is } A_{(m+1)}^{g}(k), \textit{AND} \cdots \textit{AND } \hat{y}_{(g-1)}(k) \textit{ is } A_{(m+g-1)}^{g}(k), \\ \textit{then } \hat{y}_{g}^{i}(k) \textit{ is } f_{g}^{i}(x_1(k), \cdots, x_m(k)), \hat{y}_{(g-1)}(k) \end{bmatrix} \tag{12}$$

3.3 SCFNN Optimization

The developed SCFNN model is optimized by a genetic algorithm and the least squares method. The antecedent parameters included in the fuzzy membership function are determined by a genetic algorithm and the consequent parameter vector $\mathbf{q}$ is optimized by the least squares method [3].

Furthermore, Some researchers used genetic algorithm to develop fuzzy systems, finding appropriate membership functions and fuzzy rule sets [5]. In the genetic algorithm, the following fitness function is determined to minimize root-mean-square (RMS) errors.

$$F = \exp(-\lambda(E_t + 2E_v)) \tag{13}$$

where

$$E_t = \sqrt{\frac{1}{T}\sum_{k=1}^{T}(y(k) - \hat{y}(k))^2} \tag{14}$$

$$E_v = \sqrt{\frac{1}{V}\sum_{k=T+1}^{T+V}(y(k) - \hat{y}(k))^2} \tag{15}$$

As shown in Eq. (14) and (15), T is the number of training data and V is the number of verification data.

Consequent parameter $\mathbf{q}$ is computed to minimize an objective function. This objective function is represented by the squared error between the target value $y(k)$ and the estimated value $\hat{y}(k)$.

$$J = \sum_{k=1}^{T} (y(k) - \hat{y}(k))^2 = \sum_{k=1}^{T} (y(k) - \mathbf{w}^T(k)\mathbf{q})^2 \\ = y - \hat{y} = y - \mathbf{W}\mathbf{q} \quad (16)$$

where

$$y_t = [y(1)\ y(2) \cdots y(T)]^T \quad (17)$$

4. Results of the Collapse Moment Estimation

The data obtained by performing the FEA were used to train and verify the SCFNN model to predict the collapse moment of the wall-thinned defect in the pipe bends and elbows. The result is expressed as Table II. The results show the prediction performance of the SCFNN model, which simplified the existing CFNN model, by the RMS error. The developed SCFNN model at various defect locations predicted the collapse moments for the wall-thinned defect fairly accurately.

Table II: Estimation Results of the Collapse Moments by the SCFNN Models

Defect location	Development data		Test data	
	Relative RMS error (%)	Relative Max. error (%)	Relative RMS error (%)	Relative Max. error (%)
Extrados	0.2711	2.2955	0.2890	1.1094
Intrados	0.3256	5.5831	0.4713	2.7423
Crown	0.2222	1.1112	0.4848	0.8910

5. Conclusions

In this paper, the SCFNN model was designed to estimate the collapse moment of the pipe bends and the elbows in the piping systems. The data on wall-thinned bends and elbows obtained through FEM were used to predict the collapse moment. The SCFNN model was developed and verified using independent development data and test data sets. The overall RMS errors for development and test data are less than 0.5%. The developed SCFNN model estimated the collapse moments of the bends and elbows quickly and quite accurately. Therefore, these results can be applied to assess the integrity of wall-thinned defects.

REFERENCES

[1] M. G. Na, J. W. Kim, and I. J. Hwang, Collapse Moment Estimation by Support Vector Machines for Wall-thinned Pipe Bends and Elbows, Nuclear Engineering and Design, Vol.237, p.451-459, 2007.

[2] J. W. Kim and J. G. Lee, Effect of Circumferential Location of Local Wall Thinning Defect on the Collapse Moment of Elbow, Journal of the KOSOS, Vol.201, p. 55-61, 2005.

[3] G. P. Choi, K. H. Yoo, J. H. Back, and M. G. Na, Estimation of LOCA Break Size Using Cascaded Fuzzy Neural Networks, Nuclear Engineering and Technology, Vol.49, p.495-503, 2017.

[4] D. Y. Kim, K. H. Yoo, and M. G. Na, Estimation of Minimum DNBR Using Cascaded Fuzzy Neural Networks, IEEE Transactions on Nuclear Science, Vol.62, p.1849-1856.

[5] J. C. Duan and F. L. Chung, Cascaded Fuzzy Neural Network Model Based on Syllogistic Fuzzy Reasoning, Vol.9, p.293-306, 2001.